Finite Element Analysis of Shrinkage Deformation of Light-Cured Composite Resin for Dental Restoration

Hiroyuki KINOSHITA
Department of Mechanical Systems Engineering
University of Miyazaki, Gakuenkibanadai-nishi Miyazaki 889-2192, Japan

Koichi KAIZU
Department of Mechanical and System Engineering
University of Hyogo, Shosha, Himeji 671-2280, Japan

Yoshimi OKAMURA
Faculty of Education and Culture
University of Miyazaki, Gakuenkibanadai-nishi Miyazaki 889-2192, Japan

Toshifumi YUJI
Faculty of Education and Culture
University of Miyazaki, Gakuenkibanadai-nishi Miyazaki 889-2192, Japan

Kazuo ARAKAWA
Faculty of Research Institute for Applied Mechanics
Kyushu University, 6-1 Kasuga-kouen, Fukuoka, 816-8580, Japan

Abstract- In this study, the stress distribution in the shrinkage process when a light-cured composite resin is irradiated with light was estimated. We assumed that shrinkage and hardening of the light-cured composite resin resulted from light irradiation and was the same as that caused thermally. On the basis of this assumption, we simulated the deformation during the shrinkage of the composite resin using thermal elastic-plastic finite element modeling (FEM). The simulation was carried out by changing the adhesive strength of the composite resin and the enamel. We then compared the displacement distribution of the composite resin calculated using FEM with the displacement distribution measured using the digital image correlation method. We found that the displacement distribution of the composite resin calculated using FEM agreed well with the experimental results, and we estimated the stress distribution of composite resin under these conditions. We estimated that a high tensile stress was generated in the composite resin near the corner of the cavity.

Keywords – Light-Cured Composite Resin, Shrinkage Deformation, Finite Element Analysis

I. INTRODUCTION

Light-cured composite resins are used extensively in dental restoration. They have an excellent formability and workability and their color resembles that of natural tooth. The light-cured composite resin shrinks and hardens during light irradiation. A tensile stress therefore acts near the boundary layer where the light-cured composite resin adheres to the enamel (tooth). The shrinkage stress of the composite resin caused by light irradiation separates the composite resin from the enamel because a chemical bonding force doesn't interact between the composite resin and enamel [1]. As a result, micro gaps generate between the composite resin and enamel. The micro gaps are the causes of the micro leakage [1] and separation of the composite resin from the enamel. It is very difficult to prevent completely the generation of micro gaps [2].

To prevent this from occurring, it is necessary to clarify the stress distribution during the shrinking of the light-cured composite resin. The displacement field during shrinking has already been measured using a digital image correlation method by Arakawa et al. [3-6]. However, the stress distribution in the composite resin has not been clarified yet. We therefore estimated this distribution during the shrinkage process when a light-cured composite resin was irradiated with light. Shrinkage commences at a ~470 nm wavelength. An effective method to analyze the stress of the composite resin being irradiated has not been established yet and the development of a method for clarifying its shrinkage behavior is desired.

Shrinkage with the hardening of materials also occurs thermally. For example, when melted resin is cooled, it gradually solidifies with shrinkage. We assumed that the shrinkage and hardening of the light-cured composite resin caused by light irradiation exhibited the same behavior as that caused thermally when melted resin was cooled and solidified gradually.

On the basis of this assumption, we simulated the deformation in the shrinkage of the composite resin by changing the adhesive strength of the composite resin and the enamel using thermal elastic-plastic finite element methods (FEM). We then compared the displacement distribution of the composite resin calculated using FEM with that measured using the digital image correlation method. We found that this distribution agreed well with the experimental results, and we estimated the stress distribution of the composite resin under these conditions.

II.NUMERICAL PROCEDURE

A. Finite Element Model –

As stated above, we replaced the phenomenon of shrinkage and hardening of the light-cured composite resin by light irradiation with that caused thermally, and we analyzed the deformation in the shrinkage process of the light-cured composite resin using thermal elastic-plastic FEM.

Figure 1 shows the computational model consisting of a composite resin and enamel. The composite resin is embedded in the cavity of the enamel. FEM calculations were performed using an axially symmetrical system. The model has hexahedral elements and each element has eight nodes. The number of elements for the enamel and composite resin was approximately 11000 and 8600, respectively. Lines A-B and C-D shown in Figure 1 are described later.

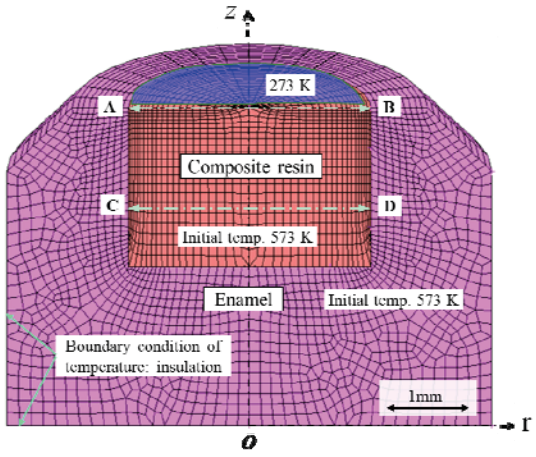

Figure 1. FEM model

B. Simulation Method and Computational Conditions –

The thermal shrinkage deformation of the composite resin was simulated using the FEM code Marc Mentat. In the simulation, equations (1) and (2) were solved simultaneously. The equation (1) gives the temperature distributions of the composite resin and enamel. The equation (2) gives relationship between temperature and stress of composite resin. An elastic-plastic deformation analysis was carried out using updated Lagrangian formulating.

$$\rho C_p \frac{\partial T}{\partial t} = \lambda\left(\frac{\partial^2 T}{\partial r^2} + \frac{1}{r}\frac{\partial T}{\partial r} + \frac{1}{r^2}\frac{\partial^2 T}{\partial \phi^2} + \frac{\partial^2 T}{\partial z^2}\right) \quad (1)$$

$$\sigma = E\alpha(\Delta T) \quad (2)$$

ρ: Density (kg / m^3), C_p: Specific heat (J・kg^{-1}・K^{-1}), T: Temperature(K), t: Time(s)

λ : Thermal conductivity (W・K^{-1}/m), E: Elastic modulus (N / m^2),
α: Coefficient of thermal expansion (K^{-1}), ΔT: Decrease in temperature (K)

Table 1 shows the physical properties of the enamel and the composite resin [7]. We assumed that the yield stress of the composite resin and the enamel was constant. We therefore analyzed them as elastic-perfectly-plastic materials without work hardening.

Table 1 Physical properties of enamel and composite resin

	Enamel	Composite resin
Young's modulus (N・ mm^{-2}) E	8.40×10^3	9.00×10^2
Yield stress (MPa) σ_0	4.00	36.4
Poisson ratio ν	0.33	0.24
Density (kg・ mm^{-3}) ρ	2.97×10^{-6}	1.60×10^{-6}
Thermal expansion (K^{-1}) α	1.14×10^{-5}	4.00×10^{-5}
Thermal conductivity (W・ K^{-1} ・ mm^{-1}) λ	9.36×10^{-4}	1.37×10^{-3}
Specific heat (J・ kg^{-1} ・K^{-1}) C_p	1000	1600

Initial and boundary conditions

We set the initial enamel and composite resin temperatures to 573 K and the outer side of the enamel to an adiabatic condition. We changed the temperature of all nodes located on the upper surface of the composite resin to 273 K. Then, we analyzed the transient deformation during the cooling of the composite resin. The values of the initial temperature for the enamel and the composite resins was determined by trial and error so that the amount of shrinkage caused by cooling the composite resin agreed roughly with that of the composite resin measured using the digital image correlation method by Arakawa et al.

Constraint conditions on adhesive strength of composite resin and enamel

The composite resin was inserted into the cavity after the enamel cavity had been coated with adhesive. The stress generated in the composite resin may change depending on the adhesive strength of the composite resin and the enamel. Therefore, we examined the influence of adhesive strength on the stress of the composite resin by setting the following three constraint conditions between the composite resin and the enamel.

Constraint condition I

When the adhesive strength of the enamel and the composite resin is strong, the composite resin that contacts the inner enamel surface cannot be separated from its surface. To set the contacting condition between the composite resin and the enamel, we used a glue contacting condition with the Marc Mentat code. The glue contacting condition does not cause a relative displacement to nodes located on the boundary surface between the composite resin and the enamel. We simulated the shrinkage deformation of the composite resin by setting all nodes of the composite resin to be in contact with the inner enamel surface as the glue contacting condition.

Constraint condition II

When the adhesive strength of the composite resin and the enamel is not very strong, the composite resin contacting the inner surface of the enamel can separate partially from its surface. We therefore simulated the shrinkage deformation by setting half the nodes of the composite resin to contact the inner enamel surface as the glue contacting condition (see Figure 2).

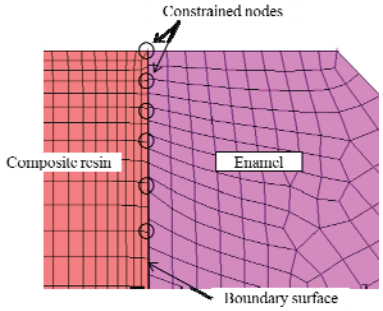

Figure 2. Nodes constrained on boundary surface between composite resin and enamel (Constraint condition II)

Constraint condition III

For the case in which the composite resin and the enamel do not adhere, the composite resin in contact with the inner enamel surface can separate from or slide on the surface. So, we simulated the shrinkage deformation without setting a constraint condition to the nodes of the composite resin in contact with the inner enamel surface.

III. Results and Discussion

A. Deformation of Composite Resin Calculated Using Each Constraint Condition –

Figure 3 shows the displacement distributions in the *r*- and *z*-directions of the composite resin calculated using each constraint condition. The temperature distribution of the composite resin and the enamel reached a steady state after approximately 30 s. Figure 3 shows the displacement distributions of the composite resin in the steady state. In all cases, the *r*-directional displacement of the composite resin was greatest near the inner enamel surface. It decreased gradually towards the inside and was zero at the center. The composite resin therefore shrinks towards the center.

In terms of the influence of the constraint conditions on the displacement distribution in the *r*-direction of the composite resin, the displacement calculated using constraint condition I was small compared with that calculated using constraint condition III, and that calculated using constraint condition II lay between the two. The displacement is thought to be small because the composite resin constrained at the inner surface of the enamel could not move freely.

The *r*-directional displacements of the composite resin that were calculated using constraint conditions I and II became the largest near their upper surface. Conversely, the *r*-directional displacement of the composite resin calculated using constraint condition III was uniform regardless of the depth direction of the cavity. For the *z*-directional displacement of the composite resin, the displacement calculated using constraint conditions I and II became the largest at the center of their upper surface. The displacement calculated using constraint condition III was uniform in the *r*-direction although it was largest at its upper surface.

B. Estimation of Stress Distribution of Composite Resin –

Figure 4 shows the displacement distributions in the *r*-direction along lines A-B and C-D of the composite resin calculated using each constraint condition (the locations of lines A-B and C-D are shown in Figure 1). The displacement measured using the digital image correlation method of Arakawa et al. is also shown.

For the displacement distribution in the *r*-direction along line A-B shown in Figure 4(a), the experimental result obtained from the measurement using the digital image correlation method indicates that the *r*-directional displacement of the composite resin becomes largest near the inner enamel surface and is zero at the center.

A comparison of the experimental results with the *r*-directional displacement calculated from FEM, shows that the displacement of the composite resin calculated using constraint condition I (glue contacting) agrees. The displacement calculated using constraint condition II (partial glue contacting) has a similar distribution to but larger displacement than the experimental result. The displacement of the composite resin calculated using constraint condition III (without constraint) does not agree with the experimental results.

For the displacement distribution in the *r*-direction along line C-D in Figure 4(b), the displacement calculated using constraint condition II has a similar distribution to that of the experimental result. The displacement distributions calculated using another constraint condition differ from those of the experimental result. It was therefore found that the result calculated under the condition that the composite resin and enamel are adhered partially exhibited a similar tendency to the experimental result.

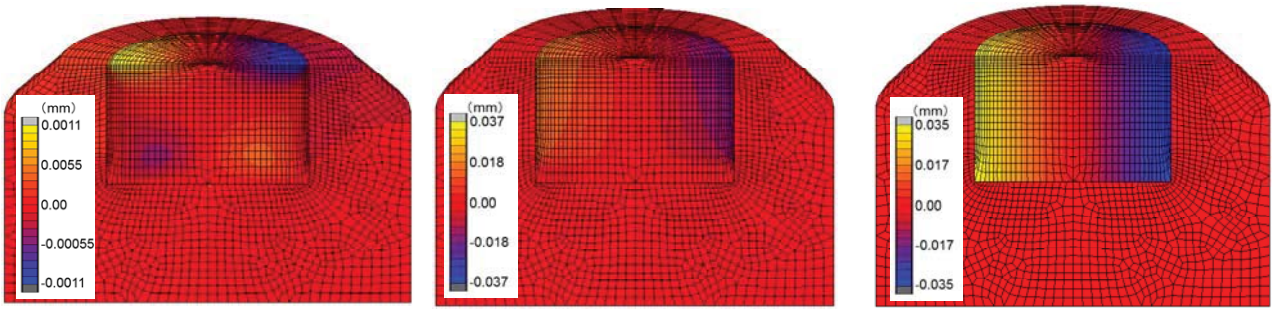

Condition I Condition II Condition III

(a) Distribution of *r*-directional displacement

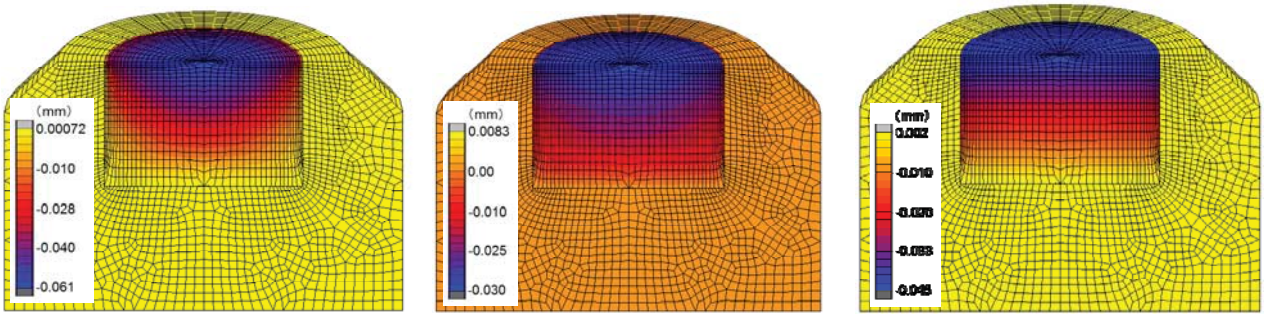

Condition I Condition II Condition III

(b) Distribution of *z*-directional displacement

Figure 3. Displacement distributions in *r*- and *z*-directions of composite resin calculated using each constraint condition

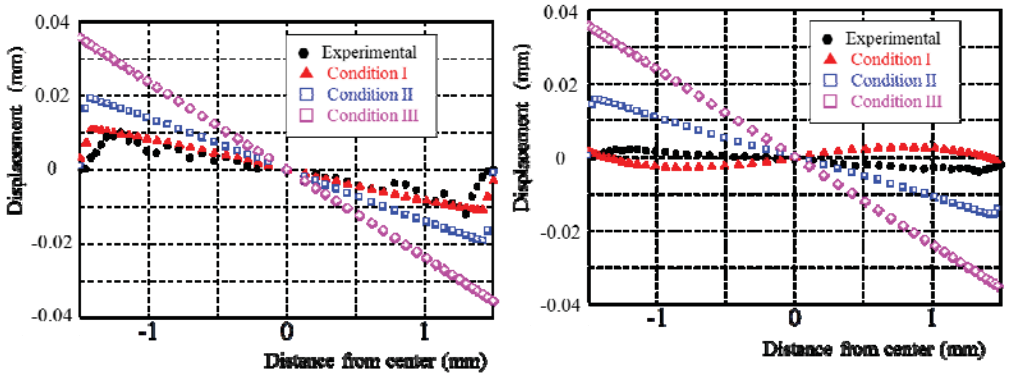

(a) Displacement along line A-B (b) Displacement along line C-D

Figure 4. Displacement distributions in *r*-direction along lines A-B and C-D of composite resin

Figure 5 shows the maximum principal stress distribution of the composite resin calculated under the condition that the composite resin and the enamel are adhered partially. A high tensile stress was generated near the corner of the cavity. From the result, it is assumed that a separation of the composite resin from the enamel occurs easily near the corner of the cavity.

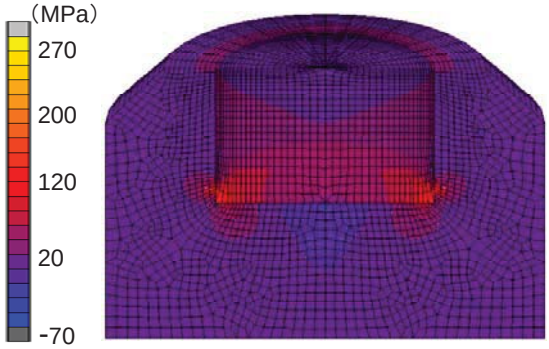

Figure 5. Maximum principal stress distribution of composite resin calculated using constraint condition II

IV. CONCLUSIONS

In this study, to estimate the stress distribution in the shrinkage process when a light-cured composite resin is irradiated with light, we simulated the deformation during shrinkage of the composite resin using thermal elastic-plastic FEM. The displacement distribution of the composite resin as calculated by FEM agreed well with that of the experimental result, and we estimated the stress distribution of the composite resin under these conditions. A high tensile stress in the composite resin was generated near the corner of the cavity.

V. ACKNOWLEDGEMENTS

Part of this work was supported by the Joint Research Laboratories of Kyushu University.

REFERENCES

[1] Kazuo ITOH, The Effect of Glazing of Composite Resin Filling, Journal of the Stomatological Society, Japan, Vol. 45, No. 3 (1978), pp. 442-453.
[2] Yuichi NAKAZAWA, Tatsuya ISHIKAWA, A Study of an Adhesive Composite Resin Restoration System (Mirage-Bond System) -Pulpal Response and Observation of Contact Area between Composite Resin and Dentinal Wall-, AD, Vol. 11, No. 1(1993), pp. 9-18.
[3] Taichi FURUKAWA, Kazuo ARAKAWA, Yasuyuki MORITA and Masakazu UCHINO, Evaluation of Shrinkage Displacement Fields in

Light Cure Composite Resin by Digital Image Correlation Method, *J. JSEM*, Vol.8, No.2 (2008), pp.115-120.
[4] Kazuo ARAKAWA, Takuto NAKANISHI, Yasuyuki MORITA and Masakazu UCHINO, Application of Digital Image Correlation Method to Water Swelling Measurement of Light Cure Composite Resin, *J. JSEM*, Vol.8, No.2 (2008), pp.115-120.
[5] Kazuo ARAKAWA, Measurement of Tooth Displacement due to Dental Occlusion using X-ray CT-images and Coordinate Transformation, *J. JSEM*, Vol.9, No.2 (2009), pp.115-120.
[6] Kazuo ARAKAWA, Yasuyuki MORITA, Masakazu UCHINO and Hirohide KAIDA, Takuto NAKANISHI, Yasuyuki MORITA and Masakazu UCHINO, Shrinkage Measurement of Light Cure Composite Resin Using Micro-focus X-ray CT images, *J. JSEM*, Vol.9, No.2 (2009), pp.115-120.
[7] Jyunji Tagami et al., Operative dentistry 21, Nagasue shoten CO. Ltd., (2011).